# Grass leaf structural and stomatal trait responses to climate gradients assessed over the 20th century and across the Great Plains, USA


## Abstract

Using herbarium specimens spanning 126 years and field-collected measurements, we assessed intraspecific trait (leaf structure and stomata) variability from grass species in the Great Plains of North America. We focused on two widespread, closely-related grasses from tribe Paniceae: *Dichanthelium oligosanthes* subsp. *scribnerianum* ($C_3$) and *Panicum virgatum* ($C_4$). Thirty-one specimens per taxon were sampled from local herbaria from the years 1887 – 2013 to assess trait responses across time to changes in atmospheric [$CO_2$] and growing season precipitation and temperature. In 2021 and 2022, the species were measured from eight grasslands sites to explore how traits vary spatially across natural continental precipitation and temperature gradients.

$\Delta^{13}C$ increased with atmospheric [$CO_2$] for *D. oligosanthes* but decreased for *P. virgatum*, likely linked to increases in precipitation in the study region over the past century. Notably, this is the first record of decreasing $\Delta^{13}C$ over time for a $C_4$ species illustrating $^{13}C$ linkages to climate. As atmospheric [$CO_2$] increased, C:N increased and $^{15}N$ decreased for both species and %N decreased for *D. oligosanthes*. Across a large precipitation gradient, *D. oligosanthes* leaf traits were more responsive to changes in precipitation than those of *P. virgatum*. In contrast, only two traits of *P. virgatum* responded to increases in temperature across a gradient: specific leaf area (increase) and leaf dry matter content (decrease). The only shared significant trend between species was increased C:N with precipitation. Our work demonstrates that these closely-related grass species with different photosynthetic pathways exhibited various trait responses across temporal and spatial scales, illustrating the key role of scale of inquiry for forecasting leaf trait responses to future environmental change.

## Introduction

Plant traits are used to predict species responses to changing environmental conditions including human-induced climate change (Violle et al., 2007; Parmesan & Hanley, 2015), shifts in nutrient cycling (Bouwman et al., 2009), and habitat loss (Helm et al., 2005). The responses of species to environmental change across space and time have consequences for understanding changes to individual water-use strategies (e.g. Voltas et al., 2015; Carlson et al., 2016; Welles & Funk, 2021), plant community composition (e.g. Jiménez et al., 2011; Cleland et al., 2013; Griffin-Nolan et al., 2019), and ecosystem-level nutrient dynamics (e.g. De Graaff et al., 2006; Campbell et al., 2009). These shifts are most commonly assessed by comparing traits across species to understand how environmental change drives shifts in community composition and ecosystem function. However, changes in the environment also impact within-species trait variation (Reich, 2014), and facilitate the existence of some species across large environmental gradients (Bachle et al., 2018). Thus, intraspecific trait variation is a key determinant forecasting responses to future environmental conditions (Violle et al., 2012), including existing spatial variation and assessments of trait responses over time (variation driven by plasticity and/or adaptation).

Since the Industrial Revolution, atmospheric $CO_2$ concentrations have increased from anthropogenic fossil fuel emissions, from around 285 parts per million (ppm) since the year 1850 (McCarroll & Loader, 2004) to over 420 ppm as of May 2022 (Keeling et al., 2005). Increased atmospheric [$CO_2$] increases plant growth and alters plant nutrient concentrations and water-use strategies (Ainsworth & Long, 2005). One major response has been the increased ratio of carbon (C) to nitrogen (N) in plant tissues over time (Peñuelas & Matamala, 1990, McLauchlan et al., 2010; McLauchlan et al., 2017; Brookshire et al., 2020; Peñuelas et al., 2020). All else equal, as atmospheric [$CO_2$] has become more readily available, plants proportionally acquire more C than other elements, such as N. This proportional stoichiometric decrease of nutrients in plant biomass has broad implications for global C and N cycling (Reich et al., 2006). As low-quality (high C:N) plant litter becomes available for decomposition by microorganisms, decomposition may slow and lead to increased immobilization or decreased rates of N mineralization, which ultimately can feed back to decrease future available N for plants (Reich et al., 2006; Welti et al.,

2020). Increases in atmospheric [$CO_2$] can also decrease soil N availability via progressive N limitation, where elevated rates of photosynthesis retain N in plant biomass (Luo et al., 2004).

Plant water-use efficiency (WUE) – the ratio of carbon fixed to water lost via stomata to the atmosphere (Farquhar et al., 1989) – tends to increase with increased atmospheric [$CO_2$]. WUE is determined by the regulation of stomatal conductance of a plant over time, coupled with the concentration gradients of $CO_2$ inside and outside of the leaf. In general, plant species have been found to have increased WUE when exposed to higher levels of [$CO_2$] (Jackson et al., 1994; Jianlin et al., 2008; Brodribb et al., 2009; Haworth et al., 2011), though the response may be optimized in angiosperms compared to other lineages, such as ferns and gymnosperms (Brodribb et al., 2009). One key indicator of changes in plant WUE over time due to increased anthropogenic $CO_2$ is a directional change in the discrimination of $^{13}C$ compared to the lighter $^{12}C$ isotope ($\Delta^{13}C$) in plant tissues. $\Delta^{13}C$ is an independent measurement of temporal changes of $\delta^{13}C$ in plant tissue over time, which is affected by decreasing levels of $^{13}C$ in atmospheric [$CO_2$] due to the burning of fossil fuels (with relatively lower amounts of $^{13}C$ compared to atmospheric [$CO_2$]) over the past two centuries (Friedli et al., 1986). Analyses of herbarium samples representing the past 200 years have found patterns of $\Delta^{13}C$ in $C_3$ plant tissue decreasing (Peñuelas & Azcón-Bieto, 1992; Pedicino et al., 2002), increasing (Zhao et al., 2001; Pedicino et al., 2002), and unchanging trends (Pedicino et al., 2002; del Toro et al., 2024). $\Delta^{13}C$ in $C_4$ plants has been found to both increase (Pedicino et al., 2002; Eastoe & Toolin, 2018; del Toro et al., 2024) and remain unchanged (Marino & McElroy, 1991; Pedicino et al., 2002) over time. These results illustrate that changes in $\Delta^{13}C$ do not reflect changes in atmospheric [$CO_2$] levels; rather, $\Delta^{13}C$ is linked more tightly to photosynthetic pathway ($C_3$ vs. $C_4$) or phylogeny (O'Leary, 1988; Farquhar et al., 1989; Stein et al., 2021). In $C_3$ plants, the bulk of carbon fractionation occurs during carboxylation by RuBisCO as this enzyme discriminates against the heavier C isotope. $\delta^{13}C$ in $C_4$ plants is less variable given that $CO_2$ is concentrated in the bundle sheath, resulting in a higher amount of $^{13}C$ fixation by RuBisCO (Farquhar et al., 1989).

Stomatal trait differences including stomatal size, density, and distribution vary among $C_3$ and $C_4$ grass species, and reflect their evolutionary history (Taylor et al. 2012; Zhao et al. 2022). Data from herbarium specimens and elevated [$CO_2$] chamber studies have revealed that some plant species reduce the number of stomata on their leaves in response to increased [$CO_2$]

(Peñuelas & Matamala, 1990; Beerling & Chaloner, 1993a; Beerling & Chaloner, 1993b; Knapp et al., 1994; Woodward & Kelly, 1995; Bettarini et al., 1998; Doheny-Adams et al., 2012; Large et al., 2017). Guard cell length (stomatal size) may also decrease (Miglietta & Raschi, 1993). With higher [$CO_2$], plants can reduce their stomatal densities to reduce water loss while maintaining similar photosynthetic production. However, this response is not uniform across all species; a wide range of species across different plant families have shown both increases or no changes in stomatal density with increases in [$CO_2$] (Beerling et al., 1992; Bettarini et al., 1998, Ydenberg et al., 2021). While herbarium specimens have been used to understand changes in non-stomatal grass leaf traits (McLauchlan et al., 2010; Brookshire et al., 2020; del Toro et al., 2024), we lack a clear understanding of how stomatal traits have changed between the varying photosynthetic pathways over recent centuries.

Many grass species have broad distributions and high abundance across large environmental gradients. Widespread distributions can be partially explained by trait plasticity that underlies tolerance to disparate environmental conditions (Siefert et al., 2015; Li et al., 2016; Moran et al., 2016; Bachle et al., 2018). On a broad scale, this may be due to plastic responses to differing environmental factors, such as precipitation, temperature, and soil characteristics (Bernard-Verdier et al., 2012; Westerband et al., 2021). Across the North American Great Plains, climate varies substantially due to precipitation and temperature gradients (Kunkel et al., 2013; Nielsen, 2018), with a cold-to-warm gradient running north to south and a dry-to-wet gradient running west to east. Previous research has shown that for both $C_3$ and $C_4$ grass species, differences in leaf traits are more often linked to precipitation than temperature gradients, with $C_4$ grasses exhibiting significantly more variability than $C_3$ grasses (Oyarzabal et al., 2008). However, it has not been tested how closely-related species with different photosynthetic pathways respond across large environmental gradients. In addition, further insight into how the traits of an individual species respond to differences in precipitation and temperature is necessary to understand how that species may respond to global change.

To assess temporal and spatial differences among traits of $C_3$ and $C_4$ grasses, we measured a suite of leaf traits (Table 1) on two closely-related (tribe Paniceae), perennial grasses: *Dichanthelium oligosanthes* subsp. *scribnerianum* ($C_3$) and *Panicum virgatum* ($C_4$). These two taxa are common throughout the Great Plains (Great Plains Flora Association, 1986)

and abundant in local herbarium collections. In this study, we evaluated how functional leaf traits of these two grasses vary over time as atmospheric [$CO_2$] has increased by measuring traits from herbarium specimens collected in Kansas. We also assessed intra-taxon variability by measuring traits at eight grassland sites across the Great Plains (Fig. 1). For temporal trends, we predicted $\Delta^{13}C$ would decrease in *D. oligosanthes* and exhibit no change in *P. virgatum*. *Dichanthelium oligosanthes* is a $C_3$ species, which we predict will respond to increased [$CO_2$] concentrations by increasing its WUE to either conserve water while maintaining the same rates of photosynthesis or increase photosynthesis and maintain the same rates of water loss, thus decreasing $\Delta^{13}C$. We did not expect $\Delta^{13}C$ of *P. virgatum* to respond over time because discrimination in $C_4$ species is minimally affected by [$CO_2$] (O'Leary, 1988). We also predicted both grasses will increase tissue C:N ratios and decrease stomatal density and stomatal lengths on both sides of the leaves in response to increased [$CO_2$] over time. Lastly, we hypothesized %N and $\delta^{15}N$ would decrease for both taxa as others have found (McLauchlan et al., 2010; McLauchlan et al., 2014 ). Because both taxa are widely distributed across North America and are known to exhibit variation in leaf morphology (Barkworth et al., 2003), we expected SLA to be greater in areas with warmer temperatures but not be correlated with differences in precipitation (Sandel et al., 2021; Griffin-Nolan & Sandel, 2023). We expect LDMC to increase with greater precipitation and decrease with higher temperatures.

## Materials and Methods

### *Collection of Herbarium Material and Field Study Sites*

To measure temporal trends in leaf traits, we sampled 14 specimens each of *D. oligosanthes* and *P. virgatum* at the Kansas State University Herbarium (KSC) and 17 specimens each at the Ronald L. McGregor Herbarium at the University of Kansas (KANU). KSC boasts a large (ca. 200,000) collection of plant specimens, many of which are historical specimens dating prior to 1900. KANU hosts approximately double (~400,000) the number of plant specimens as KSC, most of which were collected post-1950. Together these herbaria complement each other, allowing us to sample across a wider range of dates (1887 – 2013) than would have been possible at just one herbarium. For the years 2021 and 2022, plants were collected in the field and pressed and dried before sampling.

We used several criteria to standardize our sampling efforts. First, specimens needed to have ample leafy material, a prerequisite for approval for destructive sampling. Second, all specimens sampled were collected from the eastern third of the state of Kansas to minimize environmental variation by location. Third, all specimens sampled were collected during the species' respective growing season (May-July for *D. oligosanthes* and June-August for *P. virgatum*) to avoid senesced material.

To compare how *D. oligosanthes* and *P. virgatum* leaf traits vary across grasslands of the Great Plains of the United States, we sampled individuals from eight sites over the summers of 2021 and 2022 (Fig. 1): (1) Woodworth Station Waterfowl Production Area, North Dakota, (2) Cedar Creek Ecosystem Science Reserve, Minnesota, (3) Valentine National Wildlife Refuge, Nebraska, (4) T. L. Davis Preserve, Nebraska (5) Kish-Ke-Kosh Prairie, Iowa, (6) Konza Prairie Biological Station, Kansas, (7) Wah'Kon-Tah Prairie, Missouri, (8) Joseph H. Williams Tallgrass Prairie Preserve, Oklahoma. We sampled plants growing from remnant native prairies at all sites except the Woodworth Station Waterfowl Production Area, Cedar Creek Ecosystem Science Reserve, and part of Wah'Kon-Tah Prairie. At the Woodworth Station Waterfowl Production Area, all *P. virgatum* represented restored populations. At Wah'Kon-Tah Prairie, two replicates of *P. virgatum* came from restored populations. Both restored populations were seeded with locally sourced seeds. The restored populations at the Cedar Creek Ecosystem Science Reserve were recovered from the seed bank. *Dichanthelium oligosanthes* was not collected at the Woodworth Station Waterfowl Production Area and *P. virgatum* was not collected at Kish-Ke-Kosh Prairie.

*Trait Measurements*

At each grassland site, five replicates of each species (when possible) were measured for their specific leaf area (SLA), leaf dry matter content (LDMC), leaf thickness, C:N, $\delta^{13}C$, stomatal density, and stomatal length using standardized sampling methods (Pérez-Harguindeguy et al., 2016). For leaf measurements (SLA, LDMC, and leaf thickness), the most recently produced, but mature leaf was sampled from each replicate. Leaf area and leaf thickness were measured in the field. Leaf area was measured using Leafscan, a mobile app for measuring the surface area of leaves (Anderson & Rosas-Anderson, 2017), and leaf thickness using calipers.

To calculate LDMC, leaves were rehydrated by being submerged in water for 24-72 hours for wet mass measurements and dried in a drying oven at 60 °C for at least 48 hours for dry mass.

Stable isotope measurements for leaf $\delta^{13}C$, $\delta^{15}N$, total C, and total N were performed at the Stable Isotope Mass Spectrometry Laboratory at Kansas State University. Multiple leaves from each replicate were dried for at least 48 hours at 60 °C and homogenized with an amalgamator. Total C and N of homogenized leaf samples were measured using an Elementar vario Pyro cube coupled to an Elementar Vision mass spectrometer for isotope analysis. Isotopic abundance ratios were converted to δ notation using:

$$\delta = [\frac{R_{sample}}{R_{standard}} - 1] * 1000$$

where R is the ratio of heavy to light isotopes for the sample and standard, respectively. Working laboratory standards were annually calibrated against the internationally accepted standard, Vienna Pee-Dee Belemnite for $\delta^{13}C$, and atmospheric air for $\delta^{15}N$. Within-run and across-run variability of the laboratory working standard (apple leaves – NIST 1515) was < 0.05‰.

For temporal trends, all $\delta^{13}C$ values were corrected for changes in atmospheric $\delta^{13}C$ by converting to carbon isotope discrimination values $\Delta^{13}C$ according to Farquhar et al. 1982:

$$\Delta^{13}C = \frac{\delta^{13}C_{air} - \delta^{13}C_{plant}}{1 + \delta^{13}C_{plant}/1000}$$

Atmospheric [$CO_2$] and $\delta^{13}C_{air}$ measurements were retrieved from McCarroll & Loader (2004) for the years preceding 2004 and measurements from the Mauna Observatory Data were used for years 2004 – 2022 (Keeling et al., 2005).

We measured stomatal density and length using stomatal peels on herbarium samples and pressed and dried field samples collected from each study site. Stomatal peels were created by applying clear nail varnish to leaves of the specimens and peeling the varnish once dry with clear tape. Both *D. oligosanthes* and *P. virgatum* are amphistomatous, so peels were made on both the abaxial and adaxial surfaces of the leaves. For herbarium specimens, the leaves of *P. virgatum* were long and folded to fit on the mounting sheet, exposing both sides of the same leaf. Thus,

abaxial and adaxial peels were taken from the same leaf where the leaf was folded. For *D. oligosanthes*, the leaves were short and not folded to fit on the herbarium sheets, so only one side of each leaf was readily available to perform peels. To circumvent this issue, peels of the abaxial and adaxial surfaces were made on different (but similarly-developed) leaves of the same individual. For field-collected material, abaxial and adaxial peels were taken from the same leaf.

Two counts of stomatal density were taken for each peel, and five replicates of stomatal lengths were measured for each count of stomatal density (10 total per specimen). Stomata were counted under 20x magnification on the objective lens and 10x magnification on the ocular lens using an Olympus BH-2 Microscope (Shinjuku City, Tokyo, Japan). An image was taken of each leaf section using a Lumenera Infinity 2 microscopy camera (Ottawa, Canada). The area of the image field of view was determined by using a stage micrometer and was 0.120 $mm^2$ for each image. Stomatal densities were then converted to stomata per 1 $mm^2$. Total stomatal density was measured as the sum of the abaxial and adaxial stomatal densities. Stomatal length (horizontal length of the guard cell from end to end) was measuring using ImageJ; pixel length was converted to mm using a reference length determined from the stage micrometer. Five herbarium specimens of *P. virgatum* that were measured for stable isotopes were unable to be sampled for stomatal densities or lengths, as either the specimens had leaves that were too curled or wrinkled to obtain peels, or stomata were too sunken and not visible on the peels. Additionally, we note that because leaves shrink during dehydration, these measurements are likely overestimations of stomatal densities and underestimations of stomatal lengths compared to fresh leaf tissue. However, because all tissue in this study was dry, the values are all comparable.

*Statistical Analyses*

All statistical analyses were performed in R V4.2.1 (R Core Team, 2022). For temporal trait responses, we used linear regression models to determine if traits significantly differed due to changes in environmental variables over time. We performed separate linear regression for each trait (Table 1) with atmospheric [$CO_2$] (ppm) and growing season precipitation (mm) and temperature (°C) as separate predictor variables and month of collection as a random effect to account for natural changes in trait values throughout the growing season. Data for growing season (April – September) total precipitation and average temperature were retrieved from

National Oceanic and Atmospheric Administration's weather station located in Manhattan, Kansas (Lawrimore et al., 2016; Nippert, 2019). Historic precipitation and temperature data for years prior to 1891 were not available. For spatial trait responses, we used linear regression models to determine if traits significantly differed due to climactic variation in precipitation and temperature. We performed separate linear regressions for each trait (Table 1) and performed separate models using the mean 30-year growing season precipitation and the mean 30-year growing season temperature as predictor variables that characterize the local climate. These values were retrieved from the National Oceanic and Atmospheric Administration's (NOAA) U.S. Monthly Climate Normals (1991-2020) (Palecki et al., 2021) for the closest weather station to each collection site. We determined the length of the growing season for each site separately based on monthly precipitation and temperature. Mean 30-Year Growing Season Precipitation (mm) was calculated by summing the monthly precipitation normal for each month in the growing season for each site and Mean 30-Year Growing Season Temperature (°C) was calculated by averaging the monthly temperature normal for all months in the growing season for each site (Table S1). All models were performed separately for each taxon.

## Results

*Temporal Trends (from Herbarium Specimens)*

The $\Delta^{13}C$ of *D. oligosanthes* and *P. virgatum* showed opposite trends as atmospheric $[CO_2]$ increased over the 20$^{th}$ century. However, the interpretation of these trendlines indicates a similar physiological response - a decrease in WUE over time. The $\Delta^{13}C$ of *D. oligosanthes* exhibited a significant, positive correlation with atmospheric $[CO_2]$ ($R^2 = 0.09$, $P = 0.032$; Fig. 2a), and the $\Delta^{13}C$ of *P. virgatum* showed a significant, negative correlation with atmospheric $[CO_2]$ ($R^2 = 0.32$, $P < 0.001$; Fig. 2b). The %N of *D. oligosanthes* exhibited a significant, negative correlation with atmospheric $[CO_2]$ ($R^2 = 0.09$, $P = 0.002$; Fig. 2c), decreasing about 20.4% over 126 years. However, %N did not change significantly for *P. virgatum* (Fig. 2d). C:N showed significant, positive correlations with atmospheric $[CO_2]$ for both *D.* oligosanthes ($R^2 = 0.07$, $P = 0.002$; Fig. 2e) and *P. virgatum* ($R^2 = 0.14$, $P = 0.025$; Fig. 2f). On average, C:N increased about 18.7% for *D. oligosanthes* and about 41.6% for *P. virgatum* over the 126-year

period. Leaf $\delta^{15}N$ showed significant, negative correlations with atmospheric [$CO_2$] for both *D. oligosanthes* ($R^2 = 0.31$, $P < 0.001$; Fig. 2g) and *P. virgatum* ($R^2 = 0.17$, $P = 0.014$; Fig. 2h).

For stomatal traits, the abaxial stomatal length of *P. virgatum* significantly decreased as atmospheric [$CO_2$] increased ($R^2 = 0.09$, $P = 0.047$; Fig. 3h) and increased as temperature increased ($R^2 = 0.25$, $P = 0.010$; Fig. S1a). The adaxial stomatal length of *P. virgatum* significantly decreased as precipitation increased ($R^2 = 0.21$, $P = 0.019$; Fig. S1b) All other stomatal traits for both species were unchanged over time ($P > 0.05$; Fig. 3a-g).

Non-stomatal leaf traits also responded to differences in precipitation or temperature across time. The %N of *D. oligosanthes* showed a significant, negative correlation with precipitation ($R^2 = 0.18$, $P = 0.008$; Fig. S2a) and a significant, positive correlation with temperature ($R^2 = 0.10$, $P = 0.009$; Fig. S2b). C:N exhibited a significant, positive correlation with precipitation for *D. oligosanthes* ($R^2 = 0.13$, $P = 0.027$; Fig. S2c). Lastly, the $\Delta^{13}C$ of *P. virgatum* showed a significant, negative correlation with temperature ($R^2 = 0.19$, $P = 0.021$; Fig. S2d). For both species, leaf $\delta^{15}N$ did not respond to differences in precipitation or temperature across time.

*Spatial Trends (Across Grassland Sites)*

Three stomatal traits significantly decreased with increasing precipitation for *D. oligosanthes*: adaxial stomatal density ($R^2 = 0.23$, $P = 0.009$; Fig. 4e), total stomatal density ($R^2 = 0.14$, $P < 0.046$; Fig. 4f), and adaxial:abaxial stomatal ratio ($R^2 = 0.26$, $P = 0.004$; Fig. 4g). Stomatal traits did not respond to differences in temperature for *D. oligosanthes* and stomatal traits showed no responses to differences in temperature or precipitation for *P. virgatum* (Table S2).

Two structural leaf traits, SLA and C:N, increased with increasing precipitation for *D. oligosanthes* ($R^2 = 0.15$, $P = 0.013$; Fig. 4a and $R^2 = 0.20$, $P = 0.003$; Fig. 4c, respectively), whereas $\delta^{13}C$ decreased with increasing precipitation ($R^2 = 0.13$, $P = 0.022$; Fig. 4d). Leaf traits did not respond to differences in temperature for *D. oligosanthes* (Table S2). For *P. virgatum*, we found that LDMC and C:N both increased with increasing precipitation ($R^2 = 0.15$, $P = 0.023$;

Fig. 4b and $R^2 = 0.12$, $P = 0.041$; Fig. 4c, respectively). We also found that SLA decreased with increasing temperature ($R^2 = 0.31$, $P = 0.001$; Fig. 4h) and that LDMC increased with increasing temperature ($R^2 = 0.21$, $P = 0.006$; Fig. 4i) for *P. virgatum*.

## Discussion

Here, we measured a suite of leaf traits on two widespread, closely-related grasses representative of the $C_3$ (*D. oligosanthes*) and $C_4$ (*P. virgatum*) photosynthetic pathways in the Great Plains of North America. We assessed temporal (century long responses within eastern Kansas) and spatial (across the broader Great Plains of North America) variation in leaf structural and stomatal traits. While we predicted the $C_3$ species would be more sensitive to changes in $[CO_2]$ and climate over time, we found similar temporal responses in $C_3$ and $C_4$ species as both showed decreased WUE (measured by changes in $\Delta^{13}C$) and limited changes in stomatal density in response to increased atmospheric $[CO_2]$. Notably, this is the first time a decrease in $\Delta^{13}C$ has been reported for a $C_4$ species. Across the spatial gradient, we found the $C_3$ species responded more to the precipitation gradient than the $C_4$ species, while the temporal trend identified different traits and relationships for species responses to climate over the past century. These results highlight the intraspecific trait variability that exists according to environmental gradients and changes in $[CO_2]$, while also clearly illustrating that predictions of spatial trait-climate relationships in the modern record may be unsuitable for predictions of trait-climate relationships over the previous century.

### *Trait responses to changes in atmospheric $[CO_2]$ and climate since 1887*

We found limited changes in stomatal density in response to increased atmospheric $[CO_2]$ or trends in precipitation or temperature over the past 126 years. Our results are contrary to previous studies that have found decreasing stomatal densities in response to elevated $[CO_2]$ (Peñuelas & Matamala, 1990; Beerling & Chaloner, 1993a; Beerling & Chaloner, 1993b; Woodward & Kelly, 1995; Bettarini et al., 1998; Doheny-Adams et al., 2012; Large et al., 2017). Stomatal densities are generally expected to decrease with increased atmospheric $[CO_2]$ resulting in increased WUE by reducing transpiration. However, atmospheric $[CO_2]$ is not the only driver of stomatal density, which is genetically determined and sensitive to environmental conditions

during leaf maturation (Xu et al., 2016). Climate data from within the study region (Manhattan, Kansas, USA) over the last century shows a ~7% increase in mean annual precipitation and 0.93 ºC increase in mean annual temperature ([illegible]n et al., in press; Sadayappan et al., 2023). A progressively wetter and warmer climate in the region over the past century may have limited changes in stomatal density over time as decreased stomatal density and size can constrain gas exchange and limit photosynthesis and leaf cooling via transpiration (Lin et al., 2015).

Limited change in stomatal density and size in *D. oligosanthes* may explain increased $\Delta^{13}C$ over time. The $\Delta^{13}C$ of *D. oligosanthes* significantly increased with atmospheric [$CO_2$] (Fig. 2a), indicating that WUE has decreased through time in this species. Generally, $\Delta^{13}C$ is expected to decrease in $C_3$ species in response to elevated [$CO_2$] due to decreased stomatal conductance that reduces water loss without limiting photosynthetic rates (Francey & Farquhar, 1982; Peñuelas & Azcón-Bieto, 1992; Araus & Buxó, 1993; Pedicino et al., 2002). However, other studies have attributed stable $\Delta^{13}C$ over time to decreases in stomatal density, which maintains $c_i/c_a$ (ratio of intercellular to atmospheric [$CO_2$]) and $\Delta^{13}C$ under elevated [$CO_2$] (Pedicino et al., 2002; del Toro et al., 2024). We attribute the increase of $\Delta^{13}C$ in *D. oligosanthes* across the studied time period to limited changes in stomatal density corresponding with a century-long trend of increased precipitation in this region.

The negative trend of $\Delta^{13}C$ over time for *P. virgatum* indicates decreased WUE over the previous century, a response similar to the $C_3$ species (Fig. 2b,a, respectively). While few studies have measured temporal changes of $\Delta^{13}C$ in $C_4$ species, only increasing (Pedicino et al., 2002; Eastoe & Toolin, 2018; del Toro et al., 2024) and unchanging (Marino & McElroy, 1991; Pedicino et al., 2002) trends have previously been reported. To our knowledge, this is the first time a decreasing response of $\Delta^{13}C$ over time has been reported for a $C_4$ species, a finding that may be owed to little research of temporal variation of $\Delta^{13}C$ in $C_4$ plants. The $\Delta^{13}C$ of $C_4$ plants tends to increase when plants are subjected to dry or shady conditions (Buchmann et al., 1996; Fravolini et al., 2002; Ghannoum et al., 2002; Cernusak et al., 2013) or increased [$CO_2$] over time (del Toro et al. 2024). Here, it seems unlikely that the decrease in $\Delta^{13}C$ over time reflects changes in light conditions, as *P. virgatum* typically grows in full sunlight and these conditions were unchanged over time. $\Delta^{13}C$ also varies by the subtype of $C_4$ photosynthetic pathway (NAD-ME, NADP-ME, and PEP-CK) due to variation in bundle sheath leakiness. The $\Delta^{13}C$ of the

NADP-ME subtype responds the least, followed by PCK then NAD-ME (Buchmann et al., 1996). As *P. virgatum* has the NAD-ME subtype, the ~1‰ decrease observed since 1887 is reasonable. Thus, the best explanation for the changes reported here are that increased water availability and temperatures over the past century in the study region (Keen et al. in press) may be responsible for the $\Delta^{13}C$ decrease seen in *P. virgatum*. If precipitation continues to increase in the region, both *P. virgatum* and *D. oligosanthes* may be expected to continue to reduce their water use efficiency to maximize growth.

Foliar C:N was positively correlated with atmospheric [$CO_2$], suggesting *D. oligosanthes* and *P. virgatum* have responded to $CO_2$ fertilization over time (Fig. 2e,f). Plants often increase carbohydrate production more than N uptake under elevated [$CO_2$] resulting in nutrient dilution (Peñuelas & Matamala, 1990, McLauchlan et al., 2010; Feng et al., 2015; McLauchlan et al., 2017; Brookshire et al., 2020; Peñuelas et al., 2020). Changes in C:N ratios in *D. oligosanthes* were also driven by decreased %N and indicate decreased N availability despite increases in anthropogenic N deposition over this time period (McLauchlan et al., 2010; McLauchlan et al., 2014). Long-term increases in foliar C:N can limit plant N availability by decreasing foliar decomposition rates and increasing microbial N immobilization (Reich et al., 2006; Feng et al., 2015). Interestingly, changes in C:N and %N in *D. oligosanthes* showed a stronger relationship with precipitation than [$CO_2$], suggesting that directional changes in precipitation may have as large or larger impacts on plant productivity and nutrient dynamics as $CO_2$ fertilization. However, the effects of [$CO_2$] and precipitation on foliar nutrient concentrations appear to vary according to species (McLauchlan et al., 2010) and may reflect species-specific resource requirements (Craine et al., 2012) or regional climactic differences (Peñuelas et al., 2020). For example, *P. virgatum* is a highly productive species that can displace dominant grasses in areas with high water and N availability (Dybzinski & Tilman, 2007; Collins et al., 2012; Nieland & Zeglin, 2024). As *P. virgatum* has foliar C:N values nearly double that of *D. oligosanthes*, changes in species composition to more productive species would likely have more profound and lasting consequences on ecosystem nutrient dynamics than shifts in species-level C:N alone.

Foliar $\delta^{15}N$ is often positively correlated with foliar [N] and terrestrial N availability (McLauchlan et al., 2010). We found that leaf $\delta^{15}N$ significantly decreased as atmospheric [$CO_2$] increased for both species (Fig. 2g,h), which supported our hypothesis and is consistent with

previously described results from grasses, other herbaceous species, and woody species (Peñuelas & Filella, 2001; McLauchlan et al., 2010; Tang et al., 2022). In our study region, plant N availability has decreased despite increased anthropogenic N deposition since at least the 1980s (McLauchlan et al., 2014). Changes in foliar $\delta^{15}N$ over time may reflect increased N limitation as described by the progressive nitrogen limitation hypothesis – the idea that increased atmospheric [$CO_2$] causes nitrogen to become more limited in the soil due to increased N immobilization and sequestration of N by plants benefitting from elevated photosynthetic rates (Luo et al., 2004). Alternatively, changes in foliar $\delta^{15}N$ may reflect changes in the isotopic signature of N taken up by the plant rather than changes in N availability (Tang et al., 2022). Foliar depletion of $\delta^{15}N$ may be an artifact of changes to the ecosystem N signature due to N deposition (Tang et al., 2022). Decreased $\delta^{15}N$ may also reflect increased mycorrhizal activity under elevated [$CO_2$] as mycorrhizae tend to deliver depleted N to plants (McLauchlan et al., 2010; Hobbie & Högberg, 2012). While we can't determine the mechanisms driving decreased $\delta^{15}N$ in this study, it is likely this often-reported response is due to a combination of N limitation and altered N signature under environmental change.

*Trait Variation Across the Great Plains*

We measured a suite of traits on individuals of *D. oligosanthes* and *P. virgatum* across eight grassland sites located throughout of the Great Plains of North America. We predicted that we would find differences within stomatal and structural leaf traits across precipitation and temperature gradients for both grasses, as these species persist across a wide range of environments with complex temporal and spatial variability.

Species may exhibit intraspecific variation of structural leaf traits to gain competitive advantages across environmental conditions (Reich, 2014) or across climate gradients (Griffin-Nolan et al. 2018). As discussed by Griffin-Nolan & Sandel (2023), inconsistent trait responses by grass species to mean climate conditions can reflect a variety of other biotic and abiotic factors, including soil characteristics, local topography, and canopy cover. Here, we reported several leaf-traits correlated with the axes of climate variability, and a few traits that did not vary by climate. For instance, we found that *P. virgatum* decreased SLA and increased LDMC as temperature increased, whereas leaves of *D. oligosanthes* showed no differences (Fig. 4h,i). In

contrast, leaves of *D. oligosanthes* had greater SLA at wetter sites, favoring more rapid growth with increased water availability, whereas the leaves of *P. virgatum* did not change significantly (Fig. 4a). We found that *D. oligosanthes* and *P. virgatum* shared only one similar significant result across all leaf traits we measured: C:N (Fig. 4c). The increase in C:N across greater precipitation is likely due to growth dilution of N, where both grass species accrue more carbon in wetter environments and consequently dilute the abundance of N in leaves with greater area.

Though stomatal densities and sizes have been found to change across precipitation and temperature gradients (Pyakurel & Wang, 2014; Hill et al., 2015; Carlson et al., 2016; Du et al., 2021), few differences were found for the species investigated here. Stomatal traits remained unchanged for *P. virgatum* across gradients that differ in mean precipitation or temperature (Table S2). For *D. oligosanthes*, we found that adaxial and total stomatal density and stomatal ratio decreased with increasing precipitation (Fig. 4e-g). This decrease in stomatal density is likely an artifact of increasing SLA and leaf size with increasing precipitation (Fig. 4a); if the number of stomata per leaf remains constant as leaf area increases, then stomatal density will decrease.

Lastly, we also observed a decrease in $\delta^{13}C$ with increasing precipitation in *D. oligosanthes* (Fig. 4d), a trend that was previously observed in $C_3$ grasses across a precipitation gradient (Weiguo et al., 2005). In $C_3$ plants, differences in $\delta^{13}C$ are strongly driven by instantaneous $c_i/c_a$, the ratio of intracellular $[CO_2]$ to the ratio of atmospheric $[CO_2]$ (Cernusak et al., 2013). Instantaneous $c_i/c_a$ has a negative relationship with leaf $\delta^{13}C$ (Cernusak et al., 2013) and is influenced by many environmental factors including water availability, nutrient availability, irradiance, and reduced $CO_2$ partial pressures due to elevation (Tieszen, 1991). Tieszen (1991) predicted irradiance affects $c_i/c_a$ the most and water availability second, but *D. oligosanthes* was collected in open grasslands at all sites in this study, so differences in irradiance are likely unimportant as drivers of $\delta^{13}C$ in this dataset. Reduced water availability decreases $c_i/c_a$ by increasing stomatal regulation and decreasing discrimination against $^{13}C$, resulting in higher foliar $\delta^{13}C$ values (Tieszen, 1991; Cernusak et al., 2013). We conclude that it is unlikely that other factors besides growing season precipitation are driving this trend of decreasing $\delta^{13}C$ across the precipitation gradient of the Great Plains.

## Conclusion

Using a long temporal record and an extensive spatial record, we reported both similarities and unique responses to varying environmental conditions in two closely-related grass species, *D. oligosanthes* ($C_3$) and *P. virgatum* ($C_4$). Using herbarium samples, leaf $\Delta^{13}C$ suggested that both species reduced water-use efficiency in response to century-long increases in water availability. For some traits, such as stomatal density, hypothesized responses to environmental changes over the past century were not evident, which contrasts with results from other studies. When the same leaf traits were measured in field populations sampled across a north-south gradient in the Great Plains, we found that many traits, including SLA, LDMC, C:N, $\delta^{13}C$, adaxial stomatal density, total stomatal density, and stomatal ratio had statistically-significant relationships with spatial patterns of precipitation, while fewer traits (SLA and LDMC for *P. virgatum* only) had statistically-significant responses to spatial variation in temperature. These results demonstrate the importance of characterizing trait variation across both temporal and spatial scales. For instance, predictions of how $C_3$ and $C_4$ grasslands will change in the future are usually made based on the examination of the results of just a few grass species in the modern record. Our work shows that many typically held assumptions of how traits will change in response to environmental variables vary with different trait-climate relationships across space and time. If we are to understand how plants will respond to global change, especially with regard to changes in precipitation regimes, it may be necessary to first document how plants have responded to historical changes in the environment, as well as the intraspecific trait variation that currently exists.

## References

Ainsworth, E. A., & Long, S. P. (2005). What have we learned from 15 years of free-air $CO_2$ enrichment (FACE)? A meta-analytic review of the responses of photosynthesis, canopy properties and plant production to rising $CO_2$. *New Phytologist*, **165**, 351–372. https://doi.org/10.1111/j.1469-8137.2004.01224.x

Anderson, C. J. R., & Rosas-Anderson P. J. (2017). Leafscan (Version 1.3.21). [Mobile application software]. Retrieved from leafscanapp.com.

Araus, J., & Buxo, R. (1993). Changes in carbon isotope discrimination in grain cereals from the north-western Mediterranean Basin during the past seven millenia. *Functional Plant Biology*, **20**, 117–128. https://doi.org/10.1071/PP9930117

Bachle, S., Griffith, D. M., & Nippert, J. B. (2018). Intraspecific trait variability in *Andropogon gerardii*, a dominant grass species in the US Great Plains. *Frontiers in Ecology and Evolution*, 6, 1–8. https://doi.org/10.3389/fevo.2018.00217

Barkworth, M., Capels, K., Long, S., & Piep, M. (2003). Magnoliophyta: Commelinidae (in part): Poaceae (part 2). In Flora of North America Editorial Committee, (Eds.), *Flora of North America*, Vol. 25. Oxford University Press.

Beerling, D. J., Chaloner, W. G., Huntley, B., Pearson, J. A., Tooley, M. J., & Woodward, F. I. (1992). Variations in the stomatal density of *Salix herbacea* L. under the changing atmospheric $CO_2$ concentrations of late- and post-glacial time. *Philosophical Transactions of the Royal Society of London. Series B: Biological Sciences*, **336**, 215–224. https://doi.org/10.1098/rstb.1992.0057

Beerling, D. J. & Chaloner, W. G. (1993a). Stomatal density responses of Egyptian *Olea europaea* L. leaves to $CO_2$ change since 1327 BC. *Annals of Botany*, **71**, 431–435. https://doi.org/10.1006/anbo.1993.1056

Beerling, D. J. & Chaloner, W. G. (1993b). The impact of atmospheric $CO_2$ and temperature changes on stomatal density: Observation from *Quercus robur* lammas leaves. *Annals of Botany*, **71**, 231–235. https://doi.org/10.1006/anbo.1993.1029

Bernard-Verdier, M., Navas, M.-L., Vellend, M., Violle, C., Fayolle, A., & Garnier, E. (2012). Community assembly along a soil depth gradient: Contrasting patterns of plant trait convergence and divergence in a Mediterranean rangeland. *Journal of Ecology*, **100**, 1422–1433. https://doi.org/10.1111/1365-2745.12003

Bettarini, I., Vaccari, F. P., & Miglietta, F. (1998). Elevated $CO_2$ concentrations and stomatal density: Observations from 17 plant species growing in a $CO_2$ spring in central Italy. *Global Change Biology*, **4**, 17–22. https://doi.org/10.1046/j.1365-2486.1998.00098.x

Bouwman, A. F., Beusen, A. H. W., & Billen, G. (2009). Human alteration of the global nitrogen and phosphorus soil balances for the period 1970-2050: Nitrogen and phosphorous soil balances. *Global Biogeochemical Cycles*, **23**. https://doi.org/10.1029/2009GB003576

Brodribb, T. J., McAdam, S. A. M., Jordan, G. J., & Feild, T. S. (2009). Evolution of stomatal responsiveness to CO $_2$ and optimization of water-use efficiency among land plants. *New Phytologist*, **183**, 839–847. https://doi.org/10.1111/j.1469-8137.2009.02844.x

Brookshire, E. N. J., Stoy, P. C., Currey, B., & Finney, B. (2020). The greening of the Northern Great Plains and its biogeochemical precursors. *Global Change Biology*, **26**, 5404–5413. https://doi.org/10.1111/gcb.15115

Buchmann, N., Brooks, J. R., Rapp, K. D., & Ehleringer, J. R. (1996). Carbon isotope composition of $C_4$ grasses is influenced by light and water supply. *Plant, Cell and Environment*, **19**, 392–402. https://doi.org/10.1111/j.1365-3040.1996.tb00331.x

Campbell, J. L., Rustad, L. E., Boyer, E. W., Christopher, S. F., Driscoll, C. T., Fernandez, I. J., Groffman, P. M., Houle, D., Kiekbusch, J., Magill, A. H., Mitchell, M. J., & Ollinger, S. V. (2009). Consequences of climate change for biogeochemical cycling in forests of northeastern north americathis article is one of a selection of papers from ne forests 2100: A synthesis of climate change impacts on forests of the northeastern us and eastern canada. *Canadian Journal of Forest Research*, **39**, 264–284. https://doi.org/10.1139/X08-104

Carlson, J. E., Adams, C. A., & Holsinger, K. E. (2016). Intraspecific variation in stomatal traits, leaf traits and physiology reflects adaptation along aridity gradients in a South African shrub. *Annals of Botany*, **117**, 195–207. https://doi.org/10.1093/aob/mcv146

Cernusak, L. A., Ubierna, N., Winter, K., Holtum, J. A. M., Marshall, J. D., & Farquhar, G. D. (2013). Environmental and physiological determinants of carbon isotope discrimination in terrestrial plants. *New Phytologist*, **200**, 950–965. https://doi.org/10.1111/nph.12423

Cleland, E. E., Collins, S. L., Dickson, T. L., Farrer, E. C., Gross, K. L., Gherardi, L. A., Hallett, L. M., Hobbs, R. J., Hsu, J. S., Turnbull, L., & Suding, K. N. (2013). Sensitivity of grassland plant community composition to spatial vs. Temporal variation in precipitation. *Ecology*, **94**, 1687–1696. https://doi.org/10.1890/12-1006.1

Collins, S. L., Koerner, S. E., Plaut, J. A., Okie, J. G., Brese, D., Calabrese, L. B., Carvajal, A., Evansen, R. J., & Nonaka, E. (2012). Stability of tallgrass prairie during a 19-year increase in growing season precipitation. *Functional Ecology*, **26**, 1450–1459. https://doi.org/10.1111/j.1365-2435.2012.01995.x

Craine, J. M., Towne, E. G., Ocheltree, T. W., & Nippert, J. B. (2012). Community traitscape of foliar nitrogen isotopes reveals N availability patterns in a tallgrass prairie. *Plant and Soil*, **356**, 395–403. https://doi.org/10.1007/s11104-012-1141-7

De Graaff, M., Van Groenigen, K., Six, J., Hungate, B., & Van Kessel, C. (2006). Interactions between plant growth and soil nutrient cycling under elevated $CO_2$: A meta-analysis. *Global Change Biology*, **12**, 2077–2091. https://doi.org/10.1111/j.1365-2486.2006.01240.x

Del Toro, I., Case, M. F., Karp, A. T., Slingsby, J. A., & Staver, A. C. (2024). Carbon isotope trends across a century of herbarium specimens suggest $CO_2$ fertilization of $C_4$ grasses. *New Phytologist*, **243**, 560–566. https://doi.org/10.1111/nph.19868

Doheny-Adams, T., Hunt, L., Franks, P. J., Beerling, D. J., & Gray, J. E. (2012). Genetic manipulation of stomatal density influences stomatal size, plant growth and tolerance to restricted water supply across a growth carbon dioxide gradient. *Philosophical Transactions of the Royal Society B: Biological Sciences*, **367**, 547–555. https://doi.org/10.1098/rstb.2011.0272

528 Du, B., Zhu, Y., Kang, H., & Liu, C. (2021). Spatial variations in stomatal traits and their
529 coordination with leaf traits in *Quercus variabilis* across Eastern Asia. *Science of The Total*
530 *Environment*, **789**, 147757. https://doi.org/10.1016/j.scitotenv.2021.147757

531 Dybzinski, R., & Tilman, D. (2007). Resource use patterns predict long-term outcomes of plant
532 competition for nutrients and light. *The American Naturalist*, **170**, 305–318.
533 https://doi.org/10.1086/519857

534 Eastoe, C., & Toolin, L. (2018). A multi-century $\delta^{13}C$ record of the $C_4$ grass *Setaria*
535 *macrostachya* in the US Southwest: Identifying environmental causes of variability.
536 *Palaeogeography, Palaeoclimatology, Palaeoecology*, **489**, 129–136.
537 https://doi.org/10.1016/j.palaeo.2017.10.004

538 Farquhar, G. D., Ehleringer, J. R., Hubick, K. T. (1989)**.** Carbon isotope discrimination and
539 photosynthesis. *Annual Review of Plant Physiology and Plant Molecular Biology* **40**: 503– 537.
540 https://doi.org/10.1146/annurev.pp.40.060189.002443

541 Farquhar, G., O'Leary, M., & Berry, J. (1982). On the relationship between carbon isotope
542 discrimination and the intercellular carbon dioxide concentration in leaves. *Functional Plant*
543 *Biology*, **9**, 121. https://doi.org/10.1071/PP9820121

544 Feng, Z., Rütting, T., Pleijel, H., Wallin, G., Reich, P. B., Kammann, C. I., Newton, P. C. D.,
545 Kobayashi, K., Luo, Y., & Uddling, J. (2015). Constraints to nitrogen acquisition of terrestrial
546 plants under elevated $CO_2$. *Global Change Biology*, **21**, 3152–3168.
547 https://doi.org/10.1111/gcb.12938

548 Francey, R. J., & Farquhar, G. D. (1982). An explanation of $^{13}C/^{12}C$ variations in tree rings.
549 *Nature*, **297**, 28–31. https://doi.org/10.1038/297028a0

550 Fravolini, A., Williams, D. G., & Thompson T. L. (2002). Carbon isotope discrimination and
551 bundle sheath leakiness in three $C_4$ subtypes grown under variable nitrogen, water and
552 atmospheric $CO_2$ supply. *Journal of Experimental Botany*, **53**, 2261–2269.
553 https://doi.org/10.1093/jxb/erf084

554 Friedli, H., Lötscher, H., Oeschger, H., Siegenthaler, U., & Stauffer, B. (1986). Ice core record of
555 the $^{13}C/^{12}C$ ratio of atmospheric $CO_2$ in the past two centuries. *Nature*, **324**, 237–238.
556 https://doi.org/10.1038/324237a0

557 Ghannoum, O., Caemmerer, S. von, & Conroy, J. P. (2002). The effect of drought on plant water
558 use efficiency of nine NAD – ME and nine NADP – ME Australian $C_4$ grasses. *Functional Plant*
559 *Biology*, **29**, 1337. https://doi.org/10.1071/FP02056

560 Great Plains Flora Association (1986). *Flora of the Great Plains*. University Press of Kansas.

561 Griffin-Nolan, R. J., Blumenthal, D. M., Collins, S. L., Farkas, T. E., Hoffman, A. M., Mueller,
562 K. E., Ocheltree, T. W., Smith, M. D., Whitney, K. D., & Knapp, A. K. (2019). Shifts in plant
563 functional composition following long-term drought in grasslands. *Journal of Ecology*, **107**,
564 2133–2148. https://doi.org/10.1111/1365-2745.13252

565 Griffin-Nolan, R. J., Bushey, J. A., Carroll, C. J. W., Challis, A., Chieppa, J., Garbowski, M.,
566 Hoffman, A. M., Post, A. K., Slette, I. J., Spitzer, D., Zambonini, D., Ocheltree, T. W., Tissue,
567 D. T., & Knapp, A. K. (2018). Trait selection and community weighting are key to understanding
568 ecosystem responses to changing precipitation regimes. *Functional Ecology*, **32**, 1746–1756.
569 https://doi.org/10.1111/1365-2435.13135

570 Griffin-Nolan, R. J., & Sandel, B. (2023). Global intraspecific trait–climate relationships for
571 grasses are linked to a species' typical form and function. *Ecography*, **2023**, e06586.
572 https://doi.org/10.1111/ecog.06586

573 Haworth, M., Elliott-Kingston, C., & McElwain, J. C. (2011). The stomatal $CO_2$ proxy does not
574 saturate at high atmospheric $CO_2$ concentrations: Evidence from stomatal index responses of
575 Araucariaceae conifers. *Oecologia*, **167**, 11–19. https://doi.org/10.1007/s00442-011-1969-1

576 Helm, A., Hanski, I., & Pärtel, M. (2005). Slow response of plant species richness to habitat loss
577 and fragmentation. *Ecology Letters*, **9**, 72-77. https://doi.org/10.1111/j.1461-0248.2005.00841.x

578 Hill, K. E., Guerin, G. R., Hill, R. S., & Watling, J. R. (2015). Temperature influences stomatal
579 density and maximum potential water loss through stomata of *Dodonaea viscosa* subsp.
580 *angustissima* along a latitude gradient in southern Australia. *Australian Journal of Botany*, **62**,
581 657. https://doi.org/10.1071/BT14204

582 Hobbie, E. A., & Högberg, P. (2012). Nitrogen isotopes link mycorrhizal fungi and plants to
583 nitrogen dynamics. *New Phytologist*, **196**, 367–382. https://doi.org/10.1111/j.1469-
584 8137.2012.04300.x

585 Jackson, R. B., Sala, O. E., Field, C. B., & Mooney, H. A. (1994). $CO_2$ alters water use, carbon
586 gain, and yield for the dominant species in a natural grassland. *Oecologia*, **98**, 257–262.
587 https://doi.org/10.1007/BF00324212

588 Jianlin, W., Guirui, Y., Quanxiao, F., Defeng, J., Hua, Q., & Qiufeng, W. (2008). Responses of
589 water use efficiency of 9 plant species to light and CO2 and their modeling. *Acta Ecologica*
590 *Sinica*, *28*(2), 525–533. https://doi.org/10.1016/S1872-2032(08)60027-X

591 Jiménez, M. A., Jaksic, F. M., Armesto, J. J., Gaxiola, A., Meserve, P. L., Kelt, D. A., &
592 Gutiérrez, J. R. (2011). Extreme climatic events change the dynamics and invasibility of semi-
593 arid annual plant communities: Extreme events and plant invasibility. *Ecology Letters*, **14**, 1227–
594 1235. https://doi.org/10.1111/j.1461-0248.2011.01693.x

595 Keeling, C. D., Piper, S. C., Bacastow, R. B., Wahlen, M., Whorf, T. P., Heimann, M., & Meijer,
596 H. A. (2005). Atmospheric $CO_2$ and $^{13}CO_2$ exchange with the terrestrial biosphere and oceans
597 from 1978 to 2000: Observations and carbon cycle implications. In I. T. Baldwin, M. M.
598 Caldwell, G. Heldmaier, R. B. Jackson, O. L. Lange, H. A. Mooney, E.-D. Schulze, U. Sommer,
599 J. R. Ehleringer, M. Denise Dearing, & T. E. Cerling (Eds.), *A history of atmospheric $CO_2$ and*
600 *its effects on plants, animals, and ecosystems* (Vol. 177, pp. 83–113). Springer-Verlag.
601 https://doi.org/10.1007/0-387-27048-5_5

602 Keen, R.M., Sadayappan, K., Jarecke, K., Li, L., Kirk, M.F., Sullivan, P.L., Nippert, J.B., In
603 review. Unexpected hydrologic response to ecosystem state change in tallgrass prairie. *Journal*
604 *of Hydrology.*

Knapp, A. (1994). Effect of elevated $CO_2$ on stomatal density and distribution in a $C_4$ grass and a $C_3$ forb under field conditions. *Annals of Botany*, **74**, 595–599. https://doi.org/10.1006/anbo.1994.1159

Kunkel, K. E., Stevens L. E., Stevens S. E., Sun L., Janssen E., Wuebbles D., Kruk M. C., Thomas D. P., Shulski M. D., Umphlett N., Hubbard K. G., Robbins K., Romolo L., Akyuz A., Pathak T., Bergantino T. R., and Dobson J. G., 2013: Regional Climate Trends and Scenarios for the U.S. National Climate Assessment: Part 4. *Climate of the U.S. Great Plains. NOAA Technical Report NESDIS 142-4*. National Oceanic and Atmospheric Administration, National Environmental Satellite, Data, and Information Service.

Large, M. F., Nessia, H. R., Cameron, E. K., & Blanchon, D. J. (2017). Changes in stomatal density over time (1769–2015) in the New Zealand endemic tree *Corynocarpus laevigatus* J. R. Forst. & G. Forst. (Corynocarpaceae). *Pacific Science*, **71**, 319–328. https://doi.org/10.2984/71.3.6

Lawrimore, Jay H.; Ray, Ron; Applequist, Scott; Korzeniewski, Bryant; Menne, Matthew J. (2016): Global Summary of the Month (GSOM), Version 1. Manhattan, KS US (Station ID: GHCND:USC00144972). NOAA National Centers for Environmental Information. https://doi.org/10.7289/V5QV3JJ5. Accessed 9 June 2024.

Li, H., Yu, K., Ratajczak, Z., Nippert, J. B., Tondrob, D., Xu, D., Li, W., & Du, G. (2016). When variability outperforms the mean: Trait plasticity predicts plant cover and biomass in an alpine wetland. *Plant and Soil*, **407**, 401–415. https://doi.org/10.1007/s11104-016-2898-x

Lin, Y.-S., Medlyn, B. E., Duursma, R. A., Prentice, I. C., Wang, H., Baig, S., Eamus, D., De Dios, V. R., Mitchell, P., Ellsworth, D. S., De Beeck, M. O., Wallin, G., Uddling, J., Tarvainen, L., Linderson, M.-L., Cernusak, L. A., Nippert, J. B., Ocheltree, T. W., Tissue, D. T., … Wingate, L. (2015). Optimal stomatal behaviour around the world. *Nature Climate Change*, **5**, 459–464. https://doi.org/10.1038/nclimate2550

Luo, Y., Su, B., Currie, W. S., Dukes, J. S., Finzi, A., Hartwig, U., Hungate, B., Mc Murtrie, R. E., Oren, R., Parton, W. J., Pataki, D. E., Shaw, M. R., Zak, D. R., & Field, C. B. (2004).

632 Progressive nitrogen limitation of ecosystem responses to rising atmospheric carbon dioxide.
633 *BioScience*, **54**, 731. https://doi.org/10.1641/0006-3568(2004)054[0731:PNLOER]2.0.CO;2

634 Marino, B. D., & McElroy, M. B. (1991). Isotopic composition of atmospheric CO2 inferred
635 from carbon in $C_4$ plant cellulose. *Nature*, **349**, 127–131. https://doi.org/10.1038/349127a0

636 McCarroll, D., & Loader, N. J. (2004). Stable isotopes in tree rings. *Quaternary Science*
637 *Reviews*, **23**, 771–801. https://doi.org/10.1016/j.quascirev.2003.06.017

638 McLauchlan, K. K., Ferguson, C. J., Wilson, I. E., Ocheltree, T. W., & Craine, J. M. (2010).
639 Thirteen decades of foliar isotopes indicate declining nitrogen availability in central North
640 American grasslands. *New Phytologist*, **187**, 1135–1145. https://doi.org/10.1111/j.1469-
641 8137.2010.03322.x

642 McLauchlan, K. K., Craine, J. M., Nippert, J. B., & Ocheltree, T. W. (2014). Lack of
643 eutrophication in a tallgrass prairie ecosystem over 27 years. *Ecology*, **95**, 1225–1235.
644 https://doi.org/10.1890/13-1068.1

645 McLauchlan, K. K., Gerhart, L. M., Battles, J. J., Craine, J. M., Elmore, A. J., Higuera, P. E.,
646 Mack, M. C., McNeil, B. E., Nelson, D. M., Pederson, N., & Perakis, S. S. (2017). Centennial-
647 scale reductions in nitrogen availability in temperate forests of the United States. *Scientific*
648 *Reports*, **7**, 7856. https://doi.org/10.1038/s41598-017-08170-z

649 Miglietta, F., & Raschi, A. (1993). Studying the effect of elevated $CO_2$ in the open in a naturally
650 enriched environment in Central Italy. *Vegetatio*, **104–105**, 391–400.
651 https://doi.org/10.1007/BF00048168

652 Moran, E. V., Hartig, F., & Bell, D. M. (2016). Intraspecific trait variation across scales:
653 Implications for understanding global change responses. *Global Change Biology*, **22**, 137–150.
654 https://doi.org/10.1111/gcb.13000

Nieland, M. A., & Zeglin, L. H. (2024). Plant and microbial feedbacks maintain soil nitrogen legacies in burned and unburned grasslands. *Journal of Ecology*, 1365-2745.14386. https://doi.org/10.1111/1365-2745.14386

Nielsen, D. C. (2018). Influence of latitude on the US Great Plains east–west precipitation gradient. *Agricultural & Environmental Letters*, **3**, 170040. https://doi.org/10.2134/ael2017.11.0040

Nippert, J. (2019). APT02 Monthly temperature and precipitation records from Manhattan, KS *Environmental Data Initiative*, https://doi.org/10.6073/PASTA/2483E2420B65D82F23513091956138A7

O'Leary, M. H. (1988). Carbon isotopes in photosynthesis: Fractionation techniques may reveal new aspects of carbon dynamics in plants. *BioScience*, **38**, 328–336. https://doi.org/10.2307/1310735

Oyarzabal, M., Paruelo, J. M., Del Pino, F., Oesterheld, M., & Lauenroth, W. K. (2008). Trait differences between grass species along a climatic gradient in South and North America. Journal of Vegetation Science, **19**, 183–192. https://doi.org/10.3170/2007-8-18349

Palecki, M., Durre, I., Applequist, S., Arguez, A., & Lawrimore, J. (2021). *U.S. Climate Normals 2020: U.S. Hourly Climate Normals (1991-2020).* NOAA National Centers for Environmental Information.

Parmesan, C., & Hanley, M. E. (2015). Plants and climate change: Complexities and surprises. *Annals of Botany*, **116**, 849–864. https://doi.org/10.1093/aob/mcv169

Pedicino, L., Leavitt, S., Betancourt, J., & Van de Water, P. (2002). Historical variations in $\delta^{13}C$ leaf of herbarium specimens in the southwestern U.S. *Western North American Naturalist*, **62**, 348–359.

678 Peñuelas, J., & Azcon-Bieto, J. (1992). Changes in leaf $\Delta^{13}C$ of herbarium plant species during
679 the last 3 centuries of $CO_2$ increase. *Plant, Cell and Environment*, **15**, 485–489.
680 https://doi.org/10.1111/j.1365-3040.1992.tb01000.x

681 Peñuelas, J., Fernández-Martínez, M., Vallicrosa, H., Maspons, J., Zuccarini, P., Carnicer, J.,
682 Sanders, T. G. M., Krüger, I., Obersteiner, M., Janssens, I. A., Ciais, P., & Sardans, J. (2020).
683 Increasing atmospheric $CO_2$ concentrations correlate with declining nutritional status of
684 European forests. *Communications Biology*, **3**, 125. https://doi.org/10.1038/s42003-020-0839-y

685 Peñuelas, J., & Filella, I. (2001). Herbaria century record of increasing eutrophication in Spanish
686 terrestrial ecosystems. *Global Change Biology*, **7**, 427–433. https://doi.org/10.1046/j.1365-
687 2486.2001.00421.x

688 Peñuelas, J., & Matamala, R. (1990). Changes in N and S leaf content, stomatal density and
689 specific leaf area of 14 plant species during the last three centuries of $CO_2$ increase. *Journal of*
690 *Experimental Botany*, **41**, 1119–1124. https://doi.org/10.1093/jxb/41.9.1119

691 Pérez-Harguindeguy, N., Díaz, S., Garnier, E., Lavorel, S., Poorter, H., Jaureguiberry, P., Bret-
692 Harte, M. S., Cornwell, W. K., Craine, J. M., Gurvich, D. E., Urcelay, C., Veneklaas, E. J.,
693 Reich, P. B., Poorter, L., Wright, I. J., Ray, P., Enrico, L., Pausas, J. G., De Vos, A. C., …
694 Cornelissen, J. H. C. (2016). Corrigendum to: New handbook for standardised measurement of
695 plant functional traits worldwide. *Australian Journal of Botany*, **64**, 715.
696 https://doi.org/10.1071/BT12225_CO

697 PRISM Climate Group at Oregon State University. (2022). *United States Average Annual Total*
698 *Precipitation, 1991-2020 (4km; BIL)*.

699 Pyakurel, A., & Wang, J. R. (2014). Leaf Morphological and Stomatal Variations in Paper Birch
700 Populations along Environmental Gradients in Canada. *American Journal of Plant Sciences*, **05**,
701 1508–1520. https://doi.org/10.4236/ajps.2014.511166

702 R Core Team. (2022). R: A language and environment for statistical computing. R Foundation
703 for Statistical Computing.

Reich, P. B. (2014). The world-wide 'fast–slow' plant economics spectrum: A traits manifesto. *Journal of Ecology*, **102**, 275–301. https://doi.org/10.1111/1365-2745.12211

Reich, P. B., Hungate, B. A., & Luo, Y. (2006). Carbon-nitrogen interactions in terrestrial ecosystems in response to rising atmospheric carbon dioxide. *Annual Review of Ecology, Evolution, and Systematics*, **37**, 611–636. https://doi.org/10.1146/annurev.ecolsys.37.091305.110039

Sadayappan, K., Keen, R., Jarecke, K. M., Moreno, V., Nippert, J. B., Kirk, M. F., Sullivan, P. L., & Li, L. (2023). Drier streams despite a wetter climate in woody-encroached grasslands. *Journal of Hydrology*, **627**, 130388. https://doi.org/10.1016/j.jhydrol.2023.130388

Sandel, B., Pavelka, C., Hayashi, T., Charles, L., Funk, J., Halliday, F. W., Kandlikar, G. S., Kleinhesselink, A. R., Kraft, N. J. B., Larios, L., Madsen-McQueen, T., & Spasojevic, M. J. (2021). Predicting intraspecific trait variation among California's grasses. *Journal of Ecology*, **109**, 2662–2677. https://doi.org/10.1111/1365-2745.13673

Siefert, A., Violle, C., Chalmandrier, L., Albert, C. H., Taudiere, A., Fajardo, A., Aarssen, L. W., Baraloto, C., Carlucci, M. B., Cianciaruso, M. V., L. Dantas, V., Bello, F., Duarte, L. D. S., Fonseca, C. R., Freschet, G. T., Gaucherand, S., Gross, N., Hikosaka, K., Jackson, B., … Wardle, D. A. (2015). A global meta-analysis of the relative extent of intraspecific trait variation in plant communities. *Ecology Letters*, **18**, 1406–1419. https://doi.org/10.1111/ele.12508

Stein, R. A., Sheldon, N. D., & Smith, S. Y. (2021). $C_3$ plant carbon isotope discrimination does not respond to $CO_2$ concentration on decadal to centennial timescales. *New Phytologist*, **229**, 2576–2585. https://doi.org/10.1111/nph.17030

Tang, S., Liu, J., Gilliam, F. S., Hietz, P., Wang, Z., Lu, X., Zeng, F., Wen, D., Hou, E., Lai, Y., Fang, Y., Tu, Y., Xi, D., Huang, Z., Zhang, D., Wang, R., & Kuang, Y. (2022). Drivers of foliar $^{15}N$ trends in southern China over the last century. *Global Change Biology*, **28**, 5441–5452. https://doi.org/10.1111/gcb.16285

729 Taylor, S. H., Franks, P. J., Hulme, S. P., Spriggs, E., Christin, P. A., Edwards, E. J., Woodward,
730 F. I., & Osborne, C. P. (2012). Photosynthetic pathway and ecological adaptation explain
731 stomatal trait diversity amongst grasses. *New Phytologist*, **193**, 387–396.
732 https://doi.org/10.1111/j.1469-8137.2011.03935.x

733 Tieszen, L. L. (1991). Natural variations in the carbon isotope values of plants: Implications for
734 archaeology, ecology, and paleoecology. *Journal of Archaeological Science*, **18**, 227–248.
735 https://doi.org/10.1016/0305-4403(91)90063-U

736 Violle, C., Enquist, B. J., McGill, B. J., Jiang, L., Albert, C. H., Hulshof, C., Jung, V., &
737 Messier, J. (2012). The return of the variance: Intraspecific variability in community ecology.
738 *Trends in Ecology & Evolution*, **27**, 244–252. https://doi.org/10.1016/j.tree.2011.11.014

739 Violle, C., Navas, M.-L., Vile, D., Kazakou, E., Fortunel, C., Hummel, I., & Garnier, E. (2007).
740 Let the concept of trait be functional! *Oikos*, **116**, 882–892. https://doi.org/10.1111/j.0030-
741 1299.2007.15559.x

742 Voltas, J., Lucabaugh, D., Chambel, M. R., & Ferrio, J. P. (2015). Intraspecific variation in the
743 use of water sources by the circum-Mediterranean conifer *Pinus halepensis*. *New Phytologist*,
744 **208**, 1031–1041. https://doi.org/10.1111/nph.13569

745 Weiguo, L., Xiahong, F., Youfeng, N., Qingle, Z., Yunning, C., & Zhisheng, A. N. (2005). $\Delta^{13}C$
746 variation of $C_3$ and $C_4$ plants across an Asian monsoon rainfall gradient in arid northwestern
747 China. *Global Change Biology*, **11**, 1094–1100. https://doi.org/10.1111/j.1365-
748 2486.2005.00969.x

749 Welles, S. R., & Funk, J. L. (2021). Patterns of intraspecific trait variation along an aridity
750 gradient suggest both drought escape and drought tolerance strategies in an invasive herb. *Annals*
751 *of Botany*, **127**, 461–471. https://doi.org/10.1093/aob/mcaa173

752 Welti, E. A. R., Roeder, K. A., De Beurs, K. M., Joern, A., & Kaspari, M. (2020). Nutrient
753 dilution and climate cycles underlie declines in a dominant insect herbivore. *Proceedings of the*
754 *National Academy of Sciences*, **117**, 7271–7275. https://doi.org/10.1073/pnas.1920012117

Westerband, A. C., Funk, J. L., & Barton, K. E. (2021). Intraspecific trait variation in plants: A renewed focus on its role in ecological processes. *Annals of Botany*, **127**, 397–410. https://doi.org/10.1093/aob/mcab011

Woodward, F. I., & Kelly, C. K. (1995). The influence of $CO_2$ concentration on stomatal density. *New Phytologist*, **131**, 311–327. https://doi.org/10.1111/j.1469-8137.1995.tb03067.x

Xu, Z., Jiang, Y., Jia, B., & Zhou, G. (2016). Elevated-$CO_2$ response of stomata and its dependence on environmental factors. *Frontiers in Plant Science*, **7**. https://doi.org/10.3389/fpls.2016.00657

Ydenberg, R., Leyland, B., Hipfner, M., & Prins, H. H. T. (2021). Century-long stomatal density record of the nitrophyte, *Rubus spectabilis* L., from the Pacific Northwest indicates no effect of changing atmospheric carbon dioxide but a strong response to nutrient subsidy. *Ecology and Evolution*, **11**, 18081–18088. https://doi.org/10.1002/ece3.8405

Zhao, F.-J., Spiro, B., & McGrath, S. P. (2001). Trends in $^{13}C/^{12}C$ ratios and C isotope discrimination of wheat since 1845. *Oecologia*, **128**, 336–342. https://doi.org/10.1007/s004420100663

Zhao, Y.-Y., Lyu, M. A., Miao, F., Chen, G., & Zhu, X.-G. (2022). The evolution of stomatal traits along the trajectory toward $C_4$ photosynthesis. *Plant Physiology*, **190**, 441–458. https://doi.org/10.1093/plphys/kiac252

773 **Tables and Figures**

774 **Table 1:** A list of traits measured in this study.

| **Traits measured across time** | **Traits measured across space** |
|---|---|
| Total Stomatal Density (stomata/$mm^2$) | Total Stomatal Density (stomata/$mm^2$) |
| Adaxial Stomatal Density (stomata/$mm^2$) | Adaxial Stomatal Density (stomata/$mm^2$) |
| Abaxial Stomatal Density (stomata/$mm^2$) | Abaxial Stomatal Density (stomata/$mm^2$) |
| Adaxial Stomatal Length (mm) | Adaxial Stomatal Length (mm) |
| Abaxial Stomatal Length (mm) | Abaxial Stomatal Length (mm) |
| Stomatal Ratio (Adaxial:Abaxial) | Stomatal Ratio (Adaxial:Abaxial) |
| $\Delta^{13}C$ (‰) | $\delta^{13}C$ (‰) |
| C:N | C:N |
| %N | Specific Leaf Area; SLA ($cm^2\ g^{-1}$) |
| $\delta^{15}N$ | Leaf Dry Matter Content; LDMC |
| | Leaf Thickness (mm) |

775

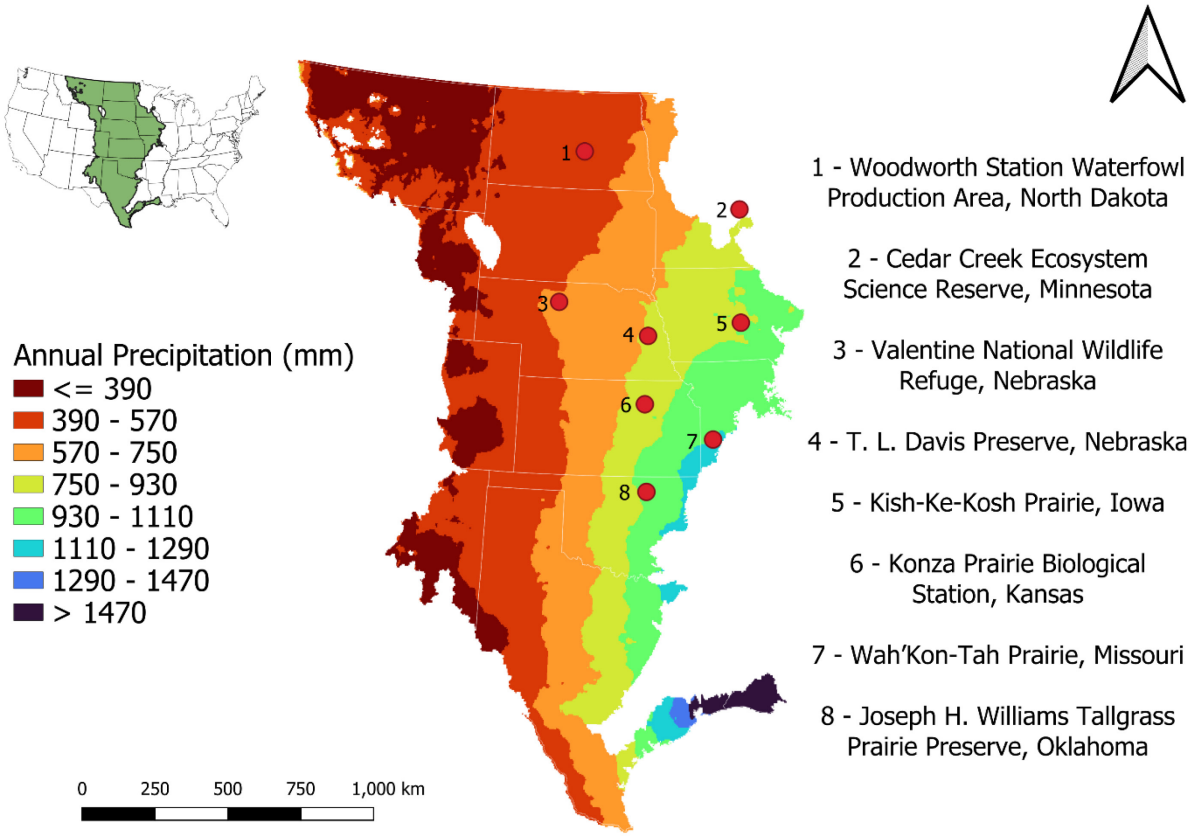


**Figure 1:** A map of the North American Great Plains ecoregion within the United States and its average annual total precipitation from 1991 – 2020. Each grassland site is represented by a red circle and each number corresponds to the site's name. We used the ecoregion boundary determined by the United States Environmental Protection Agency's Level I Ecoregions and cropped the boundary to be within the continental United States. Annual precipitation data were retrieved from the PRISM Climate Group at Oregon State University (2022).

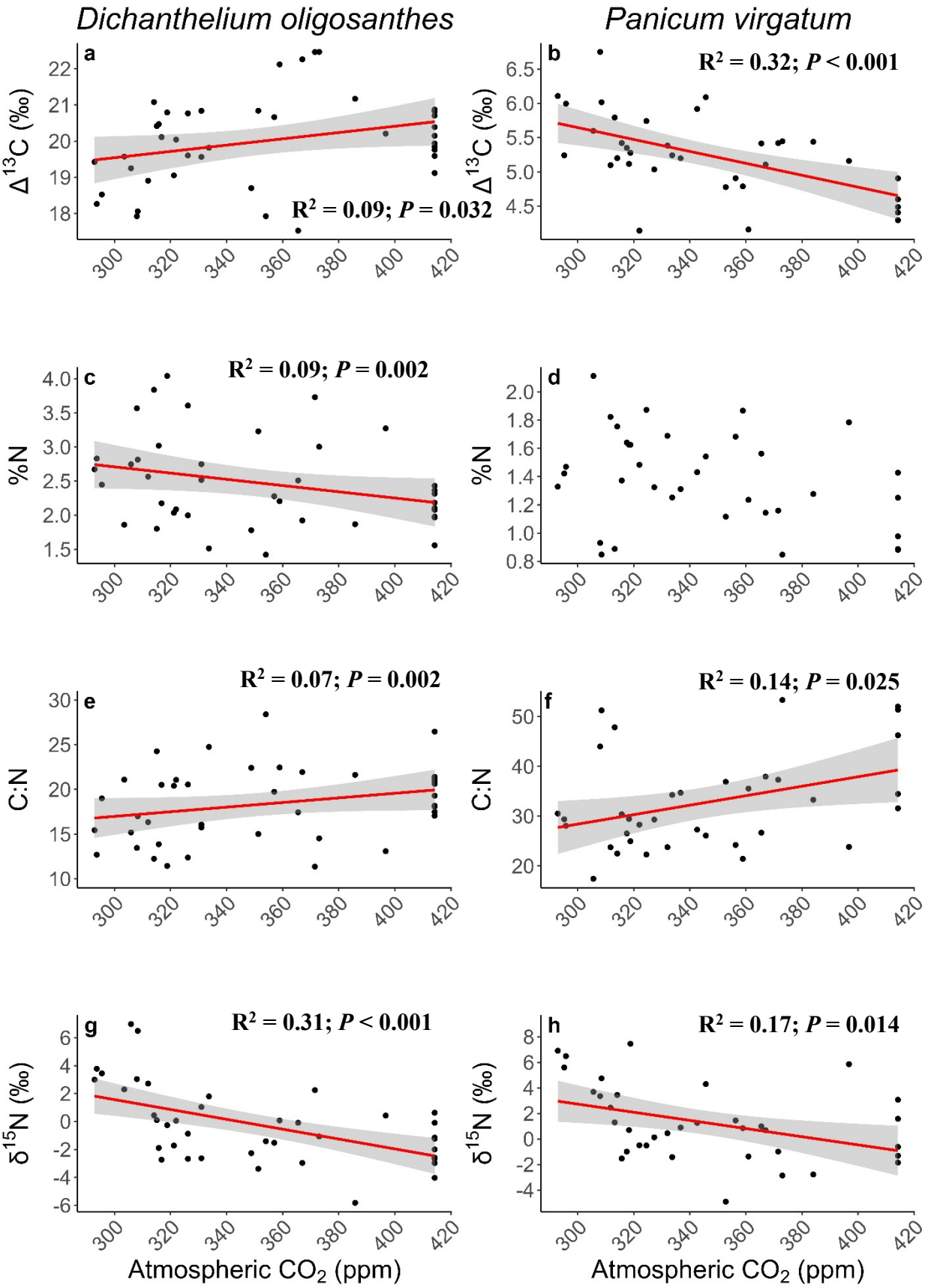
Dichanthelium oligosanthes
Panicum virgatum
a
b
c
d
e
f
g
h
$\Delta^{13}C$ (‰)
%N
C:N
$\delta^{15}N$ (‰)
$R^2 = 0.09$; $P = 0.032$
$R^2 = 0.32$; $P < 0.001$
$R^2 = 0.09$; $P = 0.002$
$R^2 = 0.07$; $P = 0.002$
$R^2 = 0.14$; $P = 0.025$
$R^2 = 0.31$; $P < 0.001$
$R^2 = 0.17$; $P = 0.014$
Atmospheric $CO_2$ (ppm)

783

**Figure 2:** The change in $\Delta^{13}C$, %N, C:N, and $\delta^{15}N$ of *D. oligosanthes* (left column) and *P. virgatum* (right column) leaves as atmospheric $CO_2$ increased from the years 1887 – 2020. Regression lines and confidence intervals are displayed when $P < 0.05$. Please note differing scales for trait values on the y-axis for both species.

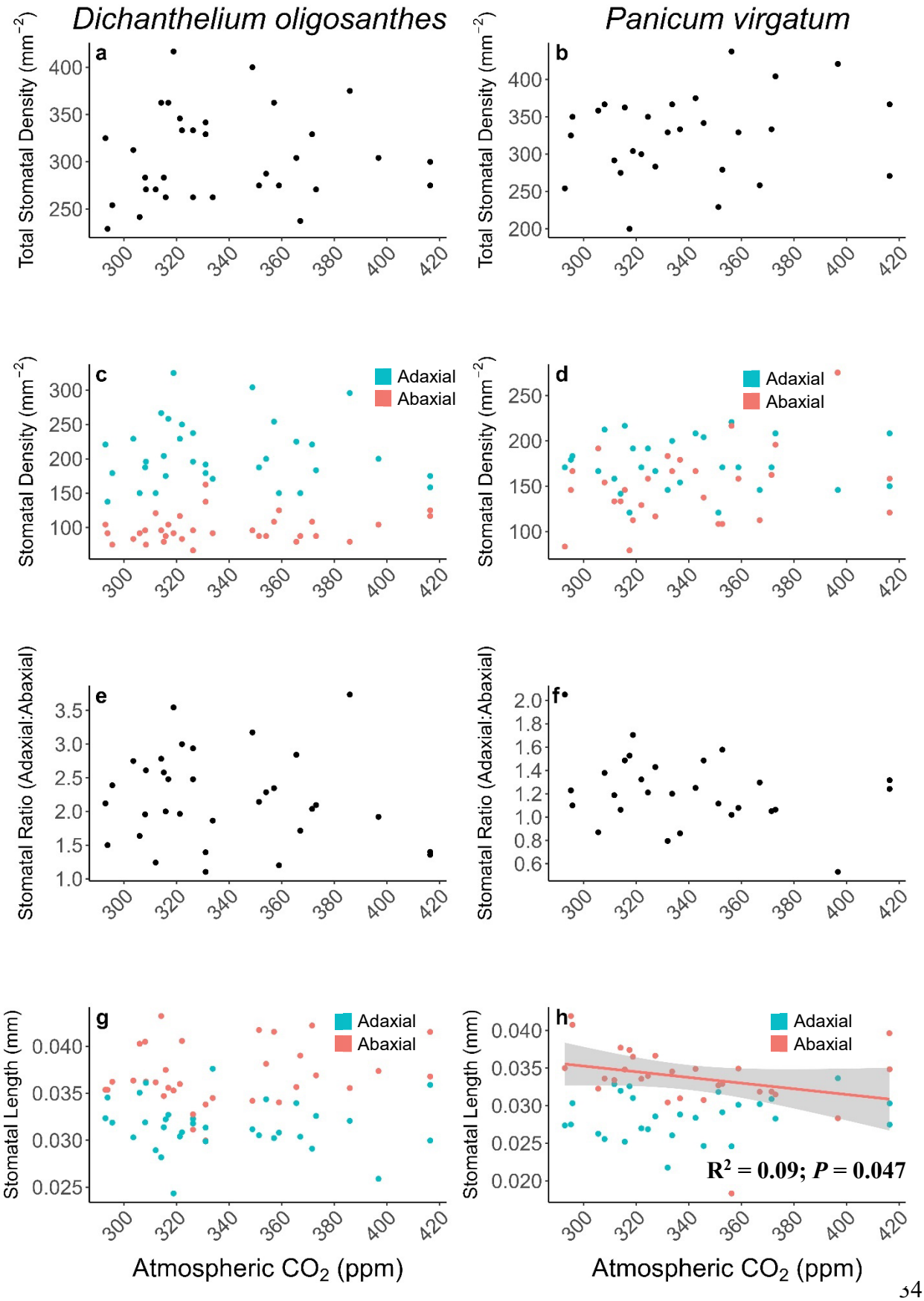
Dichanthelium oligosanthes
Panicum virgatum
a
b
c
d
e
f
g
h
Total Stomatal Density (mm$^{-2}$)
Stomatal Density (mm$^{-2}$)
Stomatal Ratio (Adaxial:Abaxial)
Stomatal Length (mm)
Adaxial
Abaxial
$R^2 = 0.09$; $P = 0.047$
Atmospheric $CO_2$ (ppm)

**Figure 3:** The change in stomatal density, stomatal ratio, and stomatal length of *D. oligosanthes* (left column) and *P. virgatum* (right column) leaves as atmospheric $CO_2$ increased from the years 1887 – 2020. Regression lines and confidence intervals are displayed when $P < 0.05$. Please note differing scales for trait values on the y-axis for both species.

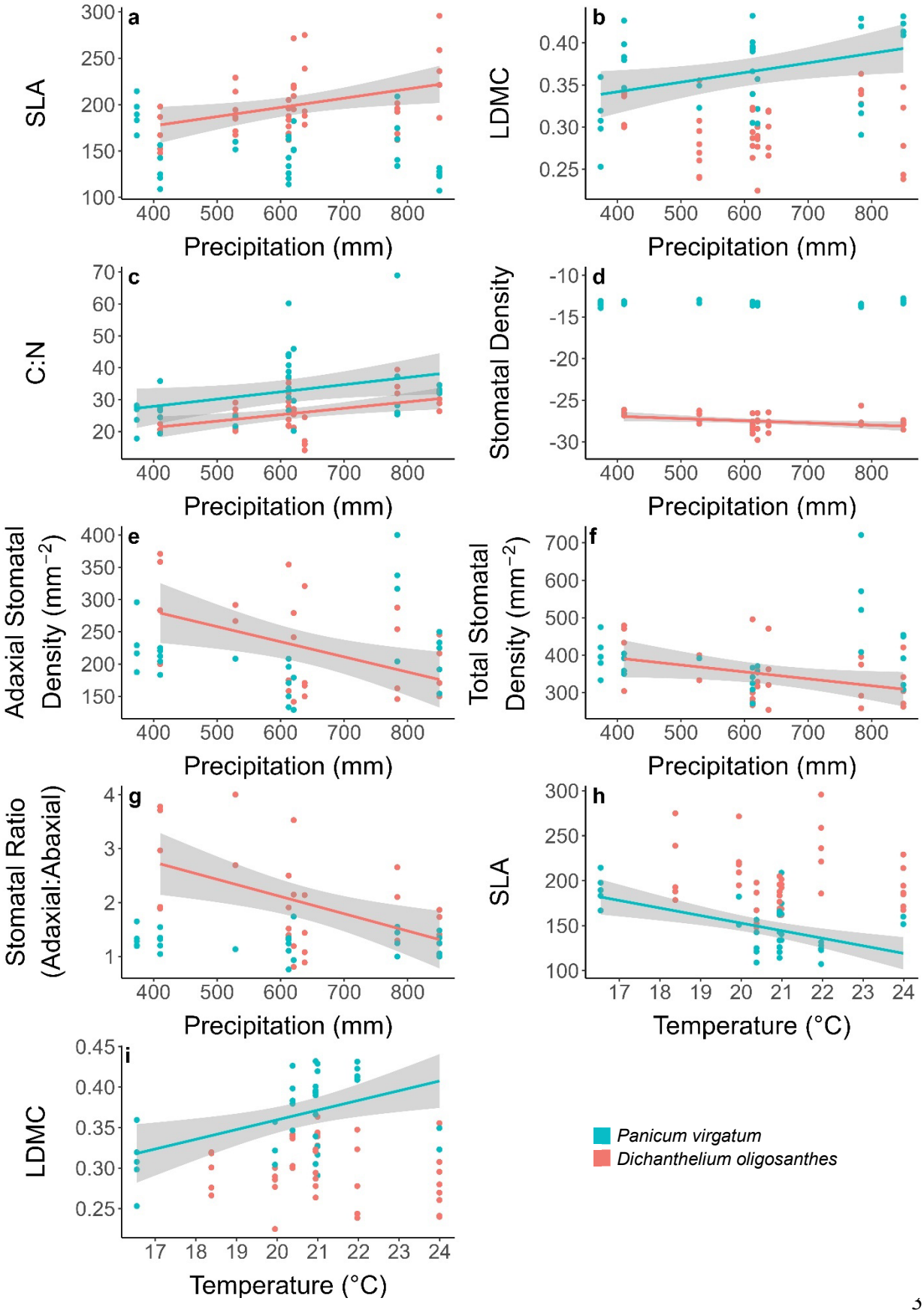
a
SLA
Precipitation (mm)
b
LDMC
Precipitation (mm)
c
C:N
Precipitation (mm)
d
Stomatal Density
Precipitation (mm)
e
Adaxial Stomatal Density (mm$^{-2}$)
Precipitation (mm)
f
Total Stomatal Density (mm$^{-2}$)
Precipitation (mm)
g
Stomatal Ratio (Adaxial:Abaxial)
Precipitation (mm)
h
SLA
Temperature (°C)
i
LDMC
Temperature (°C)
Panicum virgatum
Dichanthelium oligosanthes

793

**Figure 4:** The change of stomatal and structural leaf traits across precipitation and temperature gradients of *D. oligosanthes* (red) and *P. virgatum* (blue). Regression lines and confidence intervals are displayed when $P < 0.05$. Non-significant results for traits not displayed here can be found in Table S2.